

Fake Finger Detection Based on Time-Series Fingerprint Image Analysis

Jia Jia and Lianhong Cai

Key Laboratory of Pervasive Computing (Tsinghua University),
Ministry of Education, Beijing 100084, P.R. China
jiajia@mails.tsinghua.edu.cn,
clh-dcs@tsinghua.edu.cn

Abstract. This work introduces a new approach to detect fake fingers, based on the analysis of time-series fingerprint images. When a user puts a finger on the scanner surface, a time-series sequence of fingerprint images is captured. Five features are extracted from the image sequence. Two features represent the skin elasticity, and three features represent the physiological process of perspiration. Finally the Support Vector Matching (SVM) is used to discriminate the finger skin from other materials such as gelatin. The experiments carried out on a dataset of real and fake fingers show that the proposed approach and features are effective in fake finger detection.

1 Introduction

Fingerprint authentication (verification/identification) is one of the most important biometric technologies [1]. It has been widely used in both anti-criminal and civilian applications. However, the security of fingerprint scanners has been questioned. Previous studies have shown that fingerprint scanners can be fooled with the copies of real fingerprints which are called artificial fingerprints [2, 3]. Some approaches have been recently presented to deal with the above problem which is often referred to as “fake finger detection”, i.e. the discrimination of fake fingerprints from real ones [4, 5, 6]. Some of them use hardware-based methods to acquire life signs such as epidermis temperature, pulse oximetry, blood pressure and electric resistance [2, 5, 7]. Unfortunately, the performance achieved by most of these methods is not satisfactory, due to the inherent variability of such characteristics [6]. Furthermore, those equipments are usually expensive. Some other fake finger detection approaches use software-based methods. In [8, 9], the user is required to move the finger once it touches the scanner surface. A sequence of DistortionCodes is captured from the movement and analyzed to determine the nature of the finger. However, the way how the images are acquired is not user friendly. Another kind of methods are proposed in [4, 7, 10], which quantify a specific temporal perspiration pattern to detect fake fingers. The performances of these methods are effective [10], but they are sensitive to the different skin characteristic.

Previously, we have developed a fake finger detection method based on the analysis of finger skin elasticity [11]. It adopts the way which uses the information already

captured by the fingerprint authentication system to detect life signs. No special hardware or finger movement is required during the fingerprint acquisition process. When a user puts a finger on the scanner surface as normal fingerprint authentication system required, a time-series sequence of fingerprint images which describes the finger deformation process is captured (explained by Fig.1). Two features representing the skin elasticity are extracted from the image sequence. And the Fisher Linear Discriminant [12] is finally used to perform classification of “real finger” or “fake finger”. The testing sets contained 300 image sequences of 30 different live fingers, and 470 sequences of 47 different fake fingers. The EER of the method was 4.78%. While the initial result was encouraging, it still raised a number of issues, like the scarcity of features leads to the low adaptability of the method.



Fig. 1. A sequence of fingerprint images which describes the deformation process of a real finger

In this paper, we present the extension approach of this initial study. We use the same time-series fingerprint sequences acquisition system, and we combine two initial elasticity features with three new features which describe the physiological process of perspiration. As fake finger detection is actually a two-class classification problem, we choose the SVM [13, 14, 15] which is a powerful classifier in multi-dimensional space as our classifier.

The new proposed approach has the following advantages: 1) the time-series fingerprint sequences acquisition system is user friendly. 2) the combined features representing the skin elasticity and perspiration process have high adaptability to the variations in skin conditions. The experiments carried out on a dataset of real and fake fingers show that the proposed approach and features are effective in fake finger detection.

The rest of this paper is organized as follows. Section 2 describes the new combined features and the new classifier in detail. Section 3 gives the experimental results and the discussion. And in section 4, we give the conclusions.

2 A New Approach to Fake Finger Detection

2.1 Data Collection

When a user puts a finger on the scanner surface, we use Veridicom FPS200 capacitive scanner to capture a time-series sequence of fingerprint images at a certain frame rate. For example, when the frame rate is 20 fps (frames per second) and the capturing

duration is 1.5s, the image number of every sequence is 30. The image sequence is used for fake finger detection. One or more of them can be used for fingerprint authentication. Let $\{F_1, F_2, \dots, F_n\}$ be the sequence of n images. For each image sequence, we use the last image to compute two features which are called **static features**. And we use all the images in sequence to compute three features which are called **dynamic features**.

Our data collection method requires no extra hardware or special finger movement. Furthermore, the time-series fingerprint image sequences are used for fake finger detection while one or more of them can be used for fingerprint authentication. It's an effective way to prevent the attacker from using artificial fingerprint and real fingerprint for fake finger detection and authentication steps respectively.

2.2 Extracting the Static Features

We define two static features to describe the physiological process of finger perspiration. When in contact with the fingerprint sensor, live fingers demonstrate a distinctive moisture pattern compared to fake fingers. Capacitive fingerprint sensors are sensitive to the skin's moisture changes. Variations in gray levels of fingerprint images correspond to variations in moisture [4, 7, 10]. The static features measure periodic variability in gray level along the ridges due to the presence of perspiration around the pores. The fake fingers fail to provide the static patterns due to the lack of active pore-emanated perspiration [4].

For a time-series fingerprint image sequence, we use the last image to extract the static features. To quantify the perspiration phenomenon, we use the way described in [4] to map a 2-dimensional fingerprint image to a signal which represents the gray level values along the ridges. It contains the following steps:

Step 1: fingerprint image enhancement, which includes removing the background, smoothing the noises, and getting the binary image.

Step 2: skeleton image acquisition, which includes thinning the enhanced images to make the ridges only one pixel wide (as shown in Fig.2), discarding the curves shorter than 10 pixels since the distance between most pores is longer than 10 pixels.

Step 3: recording the gray level along the ridges and doing the Fourier transform to form a signal [4] (as shown in Fig.3).

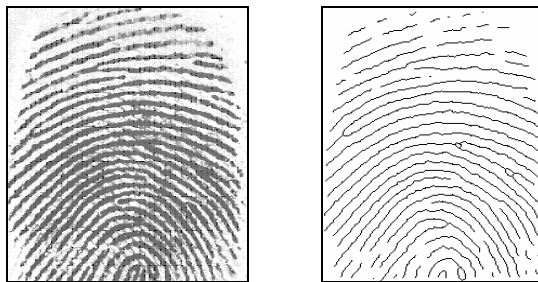


Fig. 2. A raw fingerprint image and its corresponding skeleton image

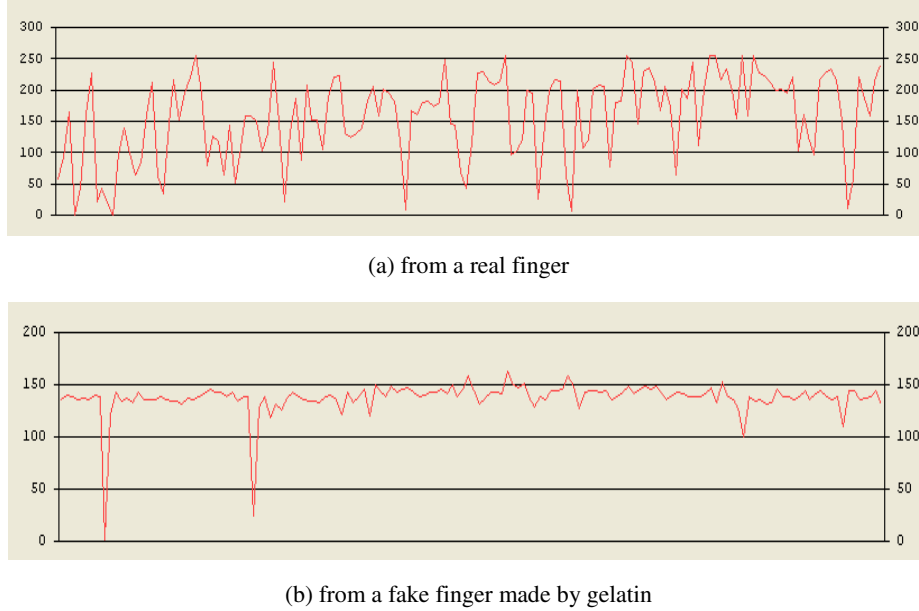


Fig. 3. The signal which represents the gray level values along the ridges of the fingerprint images

Static Feature 1 (SF1): SF1 is first mentioned in [4]. It uses the Fourier transform of the ridge signal from the last image and quantifies the existence of active pores through the corresponding spatial frequencies, as shown in Eq.1 and Eq.2.

$$f(k) = \frac{\sum_{i=1}^n \left| \sum_{p=1}^{256} L_i^a e^{-j2\pi(k-1)(p-1)/256} \right|}{n}, \quad L_i^a = L_i - \text{mean}(L_i) \quad (1)$$

$$SF1 = \sum_{k=1}^{33} f(k)^2 \quad (2)$$

where n is the total number of individual curves obtained in Step 2, and L_i represents the individual curves.

Through the observation of Fig.3, we can see that the energy of fake fingers is much lower compared to live fingers.

Static Feature 2 (SF2): SF2 describes the distribution of the signal. We divide the signal into 20 parts evenly. For each part, we record the number of pixels N_i ($i=1, 2, \dots, 20$) in raw fingerprint image whose gray level belongs to this part. SF2 is computed by Eq.3.

$$SF2 = \frac{N_{\max}}{N_{\text{all}}} \quad (3)$$

where N_{\max} represents the maximum pixel number in $\{N_i (i=1, 2, \dots, 20)\}$, and N_{all} is the sum of $N_i (i=1, 2, \dots, 20)$.

Through the observation, we can see that for the live fingers, signal distribution is much more average than fake fingers. So in most cases, the value of *SF2* of a live finger is lower than the value of a fake one.

2.3 Extracting the Dynamic Features

We define three dynamic features *DF1-DF3*. *DF1* and *DF2* describe the finger distortion process. This two features measure the finger skin elasticity. *DF3* describes the temporal change of the ridge signal from an image to the image captured 5 seconds later. The signal changes because of the propagation of the moisture between pores of real fingers. The fake fingers fail to provide the *DF3* patterns due to the lack of active pore-emanated perspiration [4].

Dynamic Feature 1 (DF1): *DF1* is the correlation coefficient of fingerprint area and signal Intensity.

For a time-series sequence $\{F_i(i=1, 2, \dots, n)\}$, the following steps are performed on each frame $F_i(i=1, 2, \dots, n)$:

We first extract the fingerprint area. Let $S_i(i=1, 2, \dots, n)$ represent the fingerprint area of $F_i(i=1, 2, \dots, n)$. Then we divide F_i into blocks of size $w \times w$ (16×16). The variance of each block is computed by Eq.4.

$$VAR = \frac{1}{w^2} \sum_{i=0}^{w-1} \sum_{j=0}^{w-1} (I(i, j) - M)^2, \quad M = \frac{1}{w^2} \sum_{i=0}^{w-1} \sum_{j=0}^{w-1} I(i, j) \quad (4)$$

where $I(i, j)$ represents the intensity (0-255) of the pixel at the i th row and j th column in one block. M represents the mean value of the block intensity. The fingerprint area S_i is obtained by Eq.5.

$$S_i = N_i \times w \times w \quad (5)$$

where N_i is the number of blocks whose *VAR* is greater than a certain threshold.

Then we compute the average signal intensity of the fingerprint area. The average signal intensity $AvgInt_i(i=1, 2, \dots, n)$ of the fingerprint area is computed by Eq.6.

$$AvgInt_i = \sum_{I(i,j) > \epsilon} I(i, j) / S_i \quad (6)$$

where $I(i, j)$ is the intensity of the pixel in fingerprint area of F_i . ϵ is a threshold which is used to separate the pixels in fingerprint area from the ones in background.

DF1 is obtained by Eq.7. It's the correlation coefficient of the fingerprint area $S=\{S_i\}(i=1,2,\dots,n)$ and the signal intensity $AvgInt=\{AvgInt_i\}(i=1,2,\dots,n)$.

$$DF1 = \frac{Cov(S, AvgInt)}{\sqrt{D(S) \times D(AvgInt)}} \quad (7)$$

where $Cov(X, Y)$ is the covariance of X and Y , and $D(X)$ is the squared deviation of X .

The signal intensity captured by a capacitive sensor is effected by two factors: the pressing pressure and the humidity of finger skin (or other materials). For a real finger, with the increase of pressure, the fingerprint area S and the signal intensity

AvgInt increases both, which means they have a positive correlation. Fig.4 shows the relation of *S* and *AvgInt* of a real finger and a fake finger made by gelatin. For real finger, with the increase of fingerprint area from 3.5 to 5.5 ($\times 10^4$), the average intensity monotonically increases from 100 to 170. But for fake finger, with the increase of fingerprint area, the average intensity presents a random fluctuation, which means they have no obvious correlation.

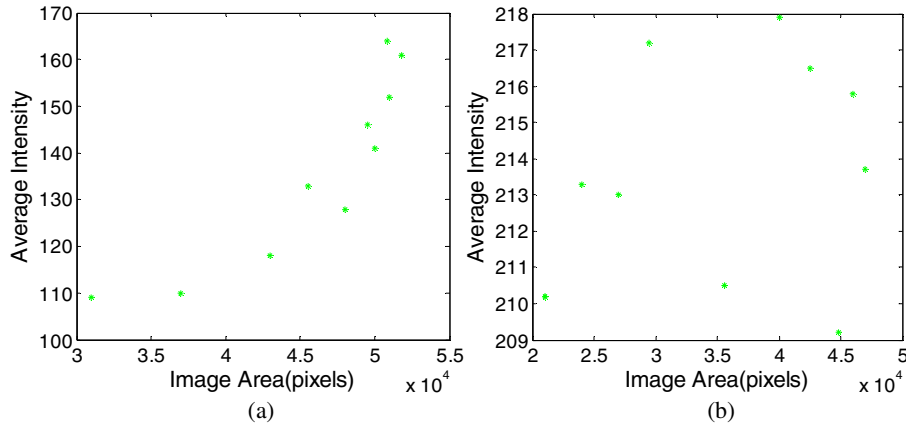


Fig. 4. The average intensity as a function of the fingerprint area. (a) a real finger, (b) a fake finger made by gelatin

Dynamic Feature 2 (DF2): DF2 is the standard deviation of fingerprint area extension in x and y axes.

For each frame F_i and its next frame F_{i+1} in a time-series sequence $\{F_i (i=1, 2, \dots, n)\}$, we compute the fingerprint area extension $Ho_i (i=1, 2, \dots, n-1)$ in x axis and $Ver_i (i=1, 2, \dots, n-1)$ in y axis, shown in Eq.8.

$$\begin{aligned}
 Ho_i &= abs(\max x_{i+1} - \min x_{i+1}) - abs(\max x_i - \min x_i) \\
 Ver_i &= abs(\max y_{i+1} - \min y_{i+1}) - abs(\max y_i - \min y_i)
 \end{aligned}
 \tag{8}$$

where x_i and y_i indicate the pixel coordinate of F_i , and $abs(x)$ is the absolute value of x .

DF2 is obtained by Eq.9. It's the mean value of the standard deviation of $H=\{Ho_i\}$ and $V=\{Ver_i\} (i=1, 2, \dots, n-1)$.

$$DF2 = \frac{1}{2} \sqrt{D(H) \times D(V)}
 \tag{9}$$

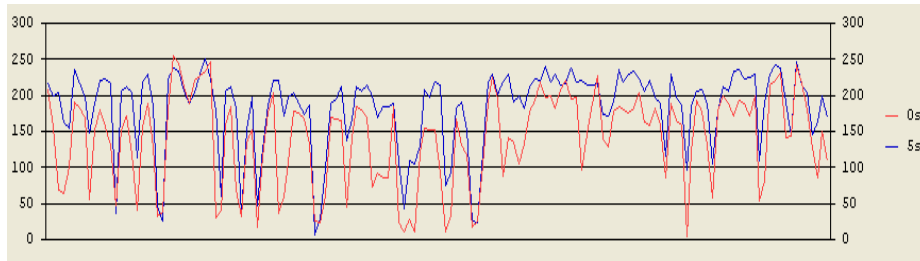
where $D(X)$ is the squared deviation of X .

Dynamic Feature 3 (DF3): DF3 is the min/max growth ratio of fingerprint signal. It is also first mentioned in [4]. We choose the image captured at the 2nd second, and the image captured 5 seconds later from the sequence $F_i (i=1, 2, \dots, n)$ to compute this

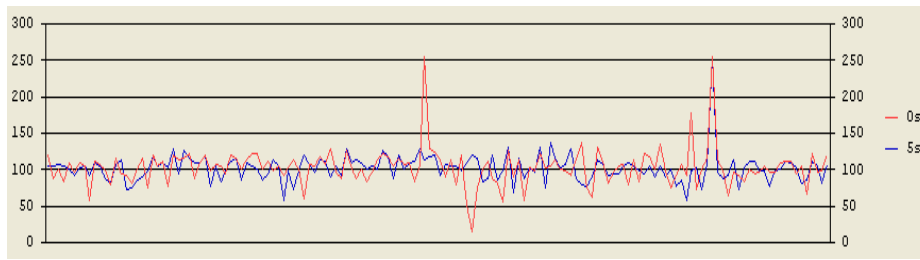
feature. Fig.5 shows the typical examples of the signal of a real finger and a fake one. $DF3$ is computed by Eq.10.

$$DF3 = \frac{\sum_j (C_{2j}^{min} - C_{1j}^{min})}{\sum_k (C_{2k}^{max} - C_{1k}^{max})} \quad (10)$$

where $C_{nj}^{min}(n=1, 2)$ represents the signal of the j th minimum point of F_n and $C_{nk}^{max}(n=1, 2)$ represents the signal of the k th maximum point of F_n .



(a) from a real finger



(b) from a fake finger made by gelatin

Fig. 5. The typical examples of the signal of a real finger and a fake one

For the live fingerprint signal, the heights of the maximums do not increase as fast as the minimums. So the average ratio of the minimum growth to maximum of two images should be lower for the live fingerprint signal compared to fake fingers [4].

2.4 Determining Results by the SVM

We define a 5-tuple feature vector $V=(SF1, SF2, DF1, DF2, DF3)$ to describe the liveness of a fingerprint sequence. As fake finger detection is actually a two-class classification problem, the SVM is chosen as the classifier. For a vector $V(SF1, SF2, DF1, DF2, DF3)$, we need to label it with “real finger” or “fake finger”. The decision function of an SVM is shown in Eq.11.

$$f(V) = \langle w \cdot V \rangle + b \quad (11)$$

where $\langle w \cdot V \rangle$ is the dot product between w (the normal vector to the hyperplane) and V (the matching vector). The margin for an input vector V_i is $y_i f(V_i)$ where $y_i \in \{-1, 1\}$ is

the correct class label for V_i . Seeking the maximum margin can be expressed as minimizing $\langle w \bullet w \rangle$ subject to $y_i(\langle w \bullet V_i \rangle + b) \geq 1, \forall i$. We allow but penalize the examples falling to the wrong side of the hyperplane.

We use SVMlight¹ for the implementation of SVM, and take linear kernel in experiments.

3 Experiments and Discussion

In this section we carried out some experiments to evaluate the presented fake fingerprint detection approach.

3.1 Datasets

In order to evaluate the proposed approach, a dataset of image sequences was collected. The dataset was acquired from 15 volunteers, all of whom were graduates of the Computer Science and Technology Department, Tsinghua University. For real fingerprints, two fingers were collected from each volunteer; ten image sequences were recorded for each real finger. For fake fingerprints, 47 fake fingers were manufactured, all of which were made of gelatin and had medium humidity; ten image sequences were recorded for each fake finger. The total number of the image sequences is 770. And the image sequences were acquired using the capacitive fingerprint scanner “Veridicom Fps200”, which produces 250×300 fingerprint images at 500 DPI.

Table 1. The information of dataset

	Different fingers/ Image sequences	Sensors	Image size	Resolution
Real fingerprint	30/300	capacitive sensor	250×300	500 dpi
Fake fingerprint	47/470	capacitive sensor	250×300	500 dpi

3.2 Measures

Let FAR (False Accept Rate) be the proportion of fake fingers that are incorrectly accepted, and FRR (False Reject Rate) be the proportion of real fingers that are incorrectly rejected. The EER (that is the value such that $FRR = FAR$) is reported as a performance indicator. Note that FAR and FRR do not include verification/identification errors. The configuration of the running computer is Pentium 2.60 GHz, 1.00GB.

3.3 Experimental Results and Discussion

For each fingerprint image sequence, we extracted the features and used the SVM to determine the final results. In our experiments, the dataset was divided into two parts: a set (400 sequences, from 15 real fingers and 25 fake fingers) used for training the classification models; and a test set (370 sequences, from the other 15 real fingers and

¹ <http://svmlight.joachims.org/>

22 fake fingers) used to measure the performance. The experimental result is shown in Fig. 6. And the EER of the proposed approach measured in the above described experimentation was 4.49%. The experimental results strongly suggest that the presented features and approach are effective in detecting fake fingers. Although it is not fair to compare our approach with other fake finger detection systems due to the difference in experimental datasets, we also list the experimental results of four different systems in Fig. 7. The first system uses extra hardware to capture the odor signal to discriminate the finger skin odor from that of other materials [6]. The second system requires user to move the finger once it touches the scanner surface; and uses a sequence of DistortionCodes to determine the nature of the finger [8]. The third system is our previous work based on the analysis of skin elasticity. And the fourth system is our new presented approach. Our new approach uses the same datasets as the third system. Obviously it is impossible for our approach to use the same datasets with the [6, 8] systems.

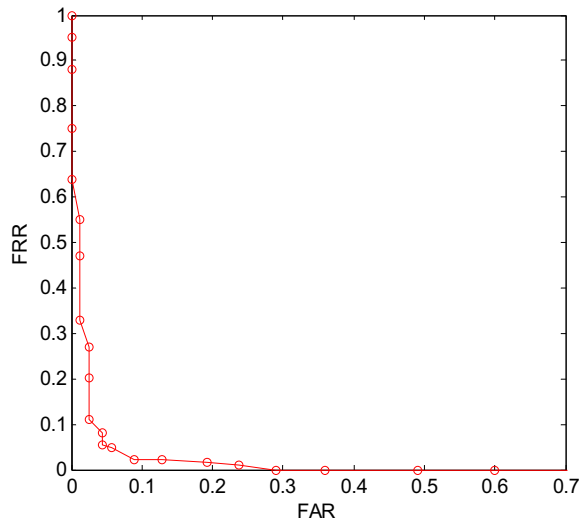


Fig. 6. The FRR as a function of FAR of the proposed approach

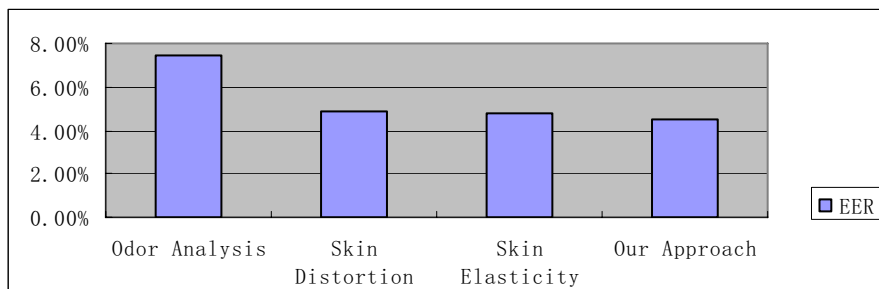


Fig. 7. The comparison of experimental results for different fake finger detection systems

4 Conclusion

Our main contributions to fake finger detection are: 1) proposing a software-based fake finger detection approach. The approach uses a user friendly way to acquire a time-series sequence of fingerprint images for each finger. The features are extracted from the image sequences and further analyzed by the SVM to determine the nature of the finger; 2) proposing a 5-tuple features representing the skin elasticity and the physiological process of perspiration. The features have strong ability in discriminating the fake fingers from real ones and high adaptability to the variations in skin conditions. The experimental results show that the proposed features and approach are effective in fake finger detection.

Acknowledgements. This research was supported by China National Natural Science Foundation (60433030, 60418012), and the Special Funds for Major State Basic Research Program of China (973 Program) (No. 2006CB303101). And I would like to thank reviewers for their kindly review and helpful comments for this paper.

References

1. Newham, E.: *The Biometric Report*. SJB Services. New York (1995)
2. Matsumoto, T., Matsumoto, H., Yamada, K., Hoshino, S.: Impact of Artificial "Gummy" Fingers on Fingerprint Systems. In *Proceeding of SPIE Vol.4677, Optical Security and Counterfeit Deterrence Techniques IV*, (2002) 275-289
3. Putte, T.v. D., Keuning, J.: Biometrical Fingerprint Recognition: Don't Get Your Fingers Burned. In *Proceeding of IFIP TC8/WG8.8 Fourth Working Conference on Smart Card Research and Advanced Applications*, (2000) 289-303
4. Derakhshani, R., Schuckers, S.A.C., Hornak, L., Gorman, L.O: Determination of Vitality from a Non-invasive Biomedical Measurement for Use in Fingerprint Scanners. *Pattern Recognition*, Vol.36(2), (2003) 383-396
5. Schuckers, S.A.C.: Spoofing and Anti-spoofing Measures. *Information Security Technical Report*, 7(4), (2002) 56-62
6. Baldisserra, D., Franco, A., Maio, D., Maltoni, D.: Fake Fingerprint Detection by Odor Analysis. In D. Zhang and A.K. Jain (Eds.): *ICB 2006, LNCS 3832*, (2005) 265-272
7. Parthasaradhi, S.T.V., Derakhshani, R., Hornak, L.A., Schuckers, S.A.C.: Time-Series Detection of Perspiration as a Liveness Test in Fingerprint Devices. *IEEE Transactions on Systems, Man, and Cybernetics-Part C: Applications and Reviews*, Vol. 35, (2005) No.3
8. Antonelli, A., Cappelli, R., Maio, D., Maltoni, D.: A New Approach to Fake Finger Detection Based on Skin Distortion. In D. Zhang and A.K. Jain (Eds.): *ICB 2006, LNCS 3832*, (2005) 221-228
9. Cappelli, R., Maio, D., Maltoni, D.: Modeling Plastic Distortion in Fingerprint Images. In *Proceedings of 2nd International Conference on Advances in Pattern Recognition (ICAPR2001)*, (2001) 369-376, Rio de Janeiro
10. Schuckers, A.C., Parthasaradhi, S.T.V., Derakhshani, R., Hornak, L.A.: Comparison of Classification Methods for Time-Series Detection of Perspiration as a Liveness Test in Fingerprint Devices. *ICBA 2004, LNCS 3072*, pp. 256-263, (2004)
11. Jia, J., Cai, L.H.: A New Approach to Fake Finger Detection Based on Skin Elasticity Analysis. Submitted to *ICB (2007)*, Seoul, Korea

12. Fisher, R.A.: The Use of Multiple Measurements in Taxonomic Problems. *Annals of Eugenics*, Vol.7, part II, (1936) 179-188
13. Cristianini, N., Shawe-Taylor, J.: *An Introduction to Support Vector Machines*. Cambridge University Press. Cambridge, UK, (2000)
14. Yuan, Y., Paolo, F., Massimiliano, P.: *Fingerprint Classification with Combinations of Support Vector Machines*. *Lecture Notes in Computer Science*, Vol. 2091. Springer-Verlag, Berlin Heidelberg New York, (2001) 253-258,
15. Joachims, T.: *Transductive Inference for Text Classification using Support Vector Machines*. In: *Proceedings of the 16th International Conference on Machine Learning (ICML)*. Bled, Slovenia, (2004) 200-209